

High-frequency (95 GHz) electron paramagnetic resonance study of the photoinduced charge transfer in conjugated polymer-fullerene composites

J. De Ceuster,¹ E. Goovaerts,¹ A. Bouwen,¹ J. C. Hummelen,² and V. Dyakonov³

¹*Physics Department, University of Antwerp, Universiteitsplein 1, B-2610 Antwerpen, Belgium*

²*Stratingh Institute and MSC, University of Groningen, Nijenborgh 4, 9747 AG Groningen, The Netherlands*

³*Energy and Semiconductor Research, University of Oldenburg, Carl von Ossietzky Str. 9-11, D-26121 Oldenburg, Germany*

(Received 12 March 2001; published 19 October 2001)

Light-induced electron paramagnetic resonance (LEPR) measurements are reported in composites of poly(2-methoxy-5-(3-,7-dimethyloctyloxy)-1,4-phenylenevinylene) (MDMO-PPV) and [6,6]-phenyl-C₆₁-butyric acid methyl ester (PCBM), a soluble derivative of C₆₀. Under illumination of the sample, two paramagnetic species are formed due to photoinduced charge transfer between conjugated polymer and fullerene. One is the positive polaron P⁺ on the polymer backbone and the other is the radical anion on the methanofullerene. Using high-frequency (95 GHz) LEPR it was possible to separate these two contributions to the spectrum on the basis of their *g* factors, and moreover to resolve the *g* anisotropy for both radicals. The positive polaron on the conjugated polymer chain possesses axial symmetry with *g* values $g_{\parallel} = 2.0034(1)$ and $g_{\perp} = 2.0024(1)$. EPR on low doped polymer gave extra proof for the assignment to the positive polaron. The negatively charged methanofullerene has a lower, rhombic symmetry with $g_x = 2.0003(1)$, $g_y = 2.0001(1)$, and $g_z = 1.9982(1)$. Different spin-lattice relaxation of both species gives rise to a rapid passage effect for the positive polaron spectrum.

DOI: 10.1103/PhysRevB.64.195206

PACS number(s): 61.82.Pv, 76.30.Rn, 76.30.-v, 61.48.+c

I. INTRODUCTION

During the last decade, interest in devices on the basis of conjugated polymers and molecules has shown an enormous increase.¹ Experimental investigation of their photophysical properties, in particular of the photogeneration of charge carriers, yields important information that can clarify the mechanism of formation and the fate of the primary excitations as well as provide a basis for photovoltaic applications. In this perspective, the existence of the photogenerated polarons, correlated polaron pairs as well as polaron (triplet) excitons, has been proven by means of photoinduced absorption (PA),²⁻⁵ optically detected magnetic resonance (ODMR),⁶⁻¹¹ and magnetic-field effect measurements.¹² Intrinsic (nonphotogenerated) polarons have also been observed in undoped conjugated systems with conventional electron paramagnetic resonance (EPR).¹³

Photogenerated charge carriers can be effectively stabilized in organic materials by doping them with electron acceptor molecules. Fullerenes act as strong electron acceptors in combination with conjugated polymers, as their lowest unoccupied molecular orbital (LUMO) lies below the excitonic state of conjugated polymers. Therefore photoinduced charge transfer occurs between them. This process occurs in the femtosecond time domain, as revealed by time-resolved spectroscopy.¹⁴⁻¹⁶ In composites of conjugated polymers and fullerenes, the existence of stable, long-living paramagnetic species can be studied by means of (cw) light-induced electron paramagnetic resonance (LEPR). X-band (9.5 GHz) LEPR measurements¹⁷⁻¹⁹ already revealed the existence of two radicals. Both overlapping contributions to the spectrum could be distinguished by different line shapes and saturation properties. One feature in the spectrum was assigned to the positive polaron formed on the polymer backbone during the

photoinduced electron transfer. The other one is the negatively charged fullerene ion, created at the same time. A recent study of the dependence of the LEPR intensity on the exciting light intensity¹⁹ revealed a bimolecular annihilation process. On the other hand, the presence of a persistent, long-living contribution to the EPR spectrum, points to the existence of electron traps in the composite. However, it was hard to resolve both contributions to the spectrum and to study the line shape of these two contributions to be able to deduce the symmetry properties of the paramagnetic molecule and the ionized conjugated segment with respect to the order within the composites. For the latter, the *g* matrix of photogenerated paramagnetic species is of importance. The symmetry and principal values of the *g* matrix are considered as one of the informative characteristics of paramagnetic centers localized/delocalized along the polymer chain and on the isolated/percolated molecules.

W-band EPR operates at a microwave frequency (95 GHz) by a factor of ten higher compared to X-band (9.5 GHz) microwaves, and at correspondingly higher resonance fields. Therefore it can more effectively separate signals on basis of their *g* values. It will also better resolve the eventual *g* anisotropy. Furthermore it has a higher absolute sensitivity as compared to X-band setup since the minimum number of detectable spins $N_{\min} \propto \nu^{-\alpha}$, where ν is the microwave frequency and $\alpha = 1.5$ or even higher,²⁰ depending on spectrometer characteristics and sample size.

Here we report on a high-frequency LEPR study of a composite of poly(2-methoxy-5-(3-,7-dimethyloctyloxy)-1,4-phenylenevinylene) (MDMO-PPV) and [6,6]-phenyl-C₆₁-butyric acid methyl ester (PCBM), a soluble derivative of C₆₀. We demonstrate that the higher resolution of this method provides additional information to the X-band measurements,¹⁷⁻¹⁹ which helps to unambiguously answer the questions about the photogeneration of independent spins.

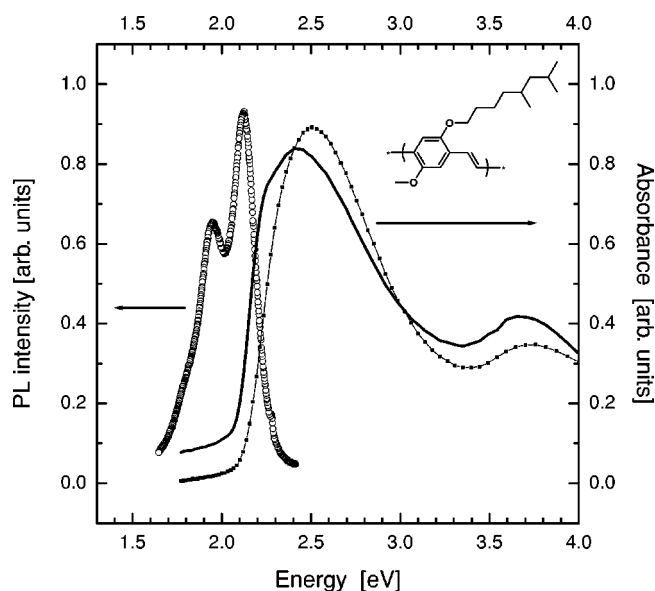


FIG. 1. Photoluminescence at room temperature (RT) (open circles) and optical absorption spectra of MDMO-PPV at RT (line with squares) and $T=77$ K (solid line). Inset shows the chemical structure.

II. EXPERIMENT

The conjugated polymer used in this investigation is poly(2-methoxy-5-(3-,7-dimethyloctyloxy)-1,4-phenylenevinylene), (MDMO-PPV). It emits in the yellow-orange region of the visible spectrum. Figure 1 shows the absorption spectrum at room temperature and 77 K and the photoluminescence (PL) spectrum, also at room temperature, of the MDMO-PPV film. In the inset to Fig. 1, the molecular structure of MDMO-PPV is given. Note the small (0.1 eV) redshift in absorption when cooling down from room temperature to 77 K, which is due to “freezing” of the molecular rotations leading to a higher degree of conjugation.²¹

The fullerene under investigation, [6,6]-phenyl- C_{61} -butyric acid methyl ester, shortly PCBM, is a C_{60} derivative with a side chain that significantly improves the molecule solubility. Figure 2 shows the optical absorption spectrum of PCBM at room temperature and the molecular structure of the molecule. The film forming properties of the PCBM are quite poor which makes absorption studies difficult due to the scattered light resulting in a strong background. The absorption across the highest occupied-lowest unoccupied molecular orbital gap, from the ground h_u state to the lowest excited state t_{1u} at 1.6–1.7 eV is parity forbidden, hence poorly observable. Around 2.4 eV, a shallow broad absorption is visible. According to Dick *et al.*,²² who studied optical absorption in pure C_{60} , this feature can be attributed to the formation of intramolecular Frenkel excitons. Similar to pure C_{60} , the UV absorption peak at around 3.7 eV is clearly visible in the PCBM. This peak may be attributed to the parity allowed transition from the h_u to the upper excited t_{1g} state.

The solid films of composites were prepared as follows. First, 1 wt % solutions of both the MDMO-PPV and PCBM were prepared separately in dimethyl-benzene (xylene),

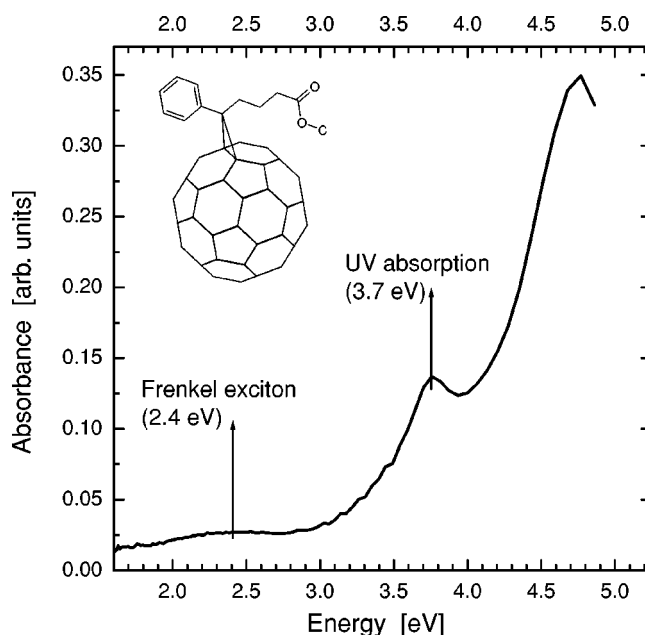


FIG. 2. Optical absorption spectrum of PCBM at RT. The chemical structure is shown in the inset.

whereafter the solutions were mixed together in a 1:1 weight ratio. Then, the composite solution was sucked in a EPR glass tube by capillary force. These tubes have an inner diameter of 0.5 mm and an outer diameter of 0.9 mm. After the solution was dried, a dense accumulation of the composite material remained close to the end of the sample tube. Samples of either pure polymer or fullerene were made for reference measurements, too.

The chemical doping of the conjugated polymer was obtained by sublimation of molecular iodine for three distinct exposure times, 10 sec, 5 min, and 4 h. The high-frequency 95 GHz (*W*-band) EPR setup consists of Bruker spectrometer (E600) with a frequency mixing bridge (9.5+84 GHz), and a Bruker cylindrical cavity, combined with an Oxford 6T superconducting magnet. For the measurements described here, the spectrometer operated with 100 kHz and 0.1 mT modulation frequency and amplitude respectively. The g values were calibrated against a powder sample of Mn^{2+} in CaO .³² The low-temperature measurements were performed in an Oxford flow cryostat (4–300 K). An optical fiber through the sample rod leads the excitation light of an Ar^+ -ion laser to the sample tube. For optical excitation, the 488 nm (≈ 2.5 eV) laser line was used. Note that this is at the peak of the absorption band of MDMO-PPV, whereas the PCBM optical absorption at this wavelength is considered to be weak. For optical absorption measurements, we used the Varian Cary 5E spectrophotometer equipped with a liquid- N_2 optical cryostat. Simulations of the EPR spectra were done with the software program EPR-NMR, developed by Mombourquette *et al.*³⁰

III. RESULTS AND DISCUSSION

The EPR powder spectrum in Fig. 3(a) demonstrates the observation of two signals in a MDMO-PPV/PCBM sample under 488 nm illumination at $T=100$ K. These signals are

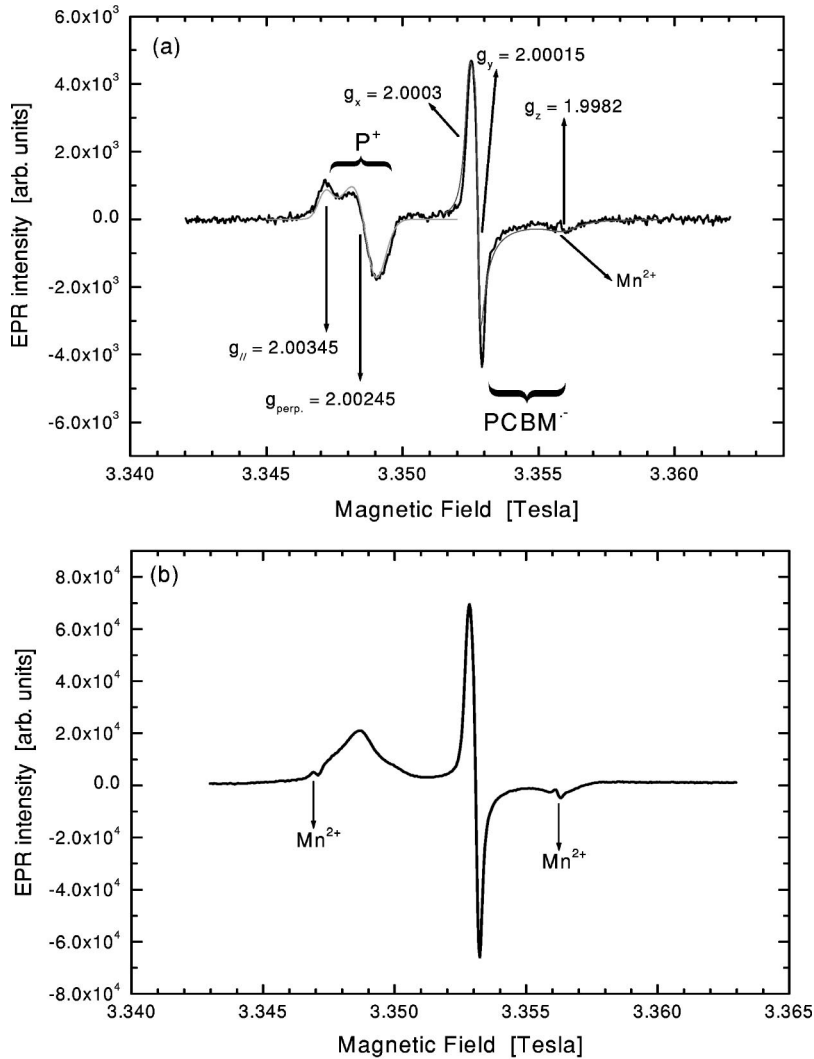


FIG. 3. (a) LEPR spectrum of the MDMO-PPV/PCBM composite, showing the methanofullerene radical (PCBM⁻), and the positive polaron (P⁺). ($P_{\mu w} = 3 \times 10^{-7}$ mW, $T = 100$ K, $\lambda_{exc.} = 488$ nm). The thin lines are simulations. (b) LEPR spectrum of the MDMO-PPV/PCBM composite in fast passage regime. ($P_{\mu w} = 3 \times 10^{-5}$ mW, $T = 100$ K, $\lambda_{exc.} = 488$ nm). Weak spurious Mn²⁺ lines originating from the cavity are indicated in both spectra.

denoted by P⁺ and PCBM⁻. The first one originates from the positively charged polaron with spin $S = 1/2$ formed on the polymer backbone and the latter originates from the negatively charged methanofullerene (also with $S = 1/2$). We did not observe any EPR signals in pure MDMO-PPV without optical excitation, and this indicates a high purity of the polymer with only few chain defects. This is different from the situation described in Ref. 13 where “dark” EPR signals from positive polarons in conjugated polymer were detectable. In pure MDMO-PPV, however, we were able to detect a weak signal under illumination. This is an indication of interchain charge transfer, which was also demonstrated in ODMR studies of pure conjugated polymers.^{10,11} In contrast, there is a weak dark signal at $g = 2.0022(1)$ found in pure PCBM at very low microwave power (not shown). The origin of this signal is ambiguous. It could point to the presence of impurities, chemical residuals, or a radical formed on the phenyl side group. The ground-state intramolecular charge transfer between the methanofullerene and the side chain is less likely to occur, otherwise it would result in at least one EPR signal with the g value below the free electron value $g_0 = 2.002319$ as it is found in other C₆₀ based compounds.^{23,24}

According to the spectrum shown in Fig. 3(a), the P⁺ has axial symmetry with g values $g_{\parallel} = 2.0034(1)$ and $g_{\perp} = 2.0024(1)$. The best fit of the P⁺ signal was achieved using a Gaussian line shape, which means that the transitions are inhomogeneously broadened, most likely due to unresolved hyperfine interaction of unpaired spin with protons. There are two effects to be discussed here. The deviation from g_0 of the g factor of such aromatic radicals in conjugated π -electron systems is due to noncompensated orbital momentum, which induces an additional magnetic field. In Ref. 25 this is explained as the consequence of $\sigma \rightarrow \pi \rightarrow \sigma^*$ excitations. The deviation Δg of the g factor from the free-electron value, depends on the spin-orbit coupling λ and the energy differences between the σ and π levels, ΔE_1 , and between the π and σ^* levels, ΔE_2 :

$$\Delta g = -\frac{\lambda}{3} \left(\frac{1}{\Delta E_1} - \frac{1}{\Delta E_2} \right).$$

The orbital moment due to a direct π - π^* excitation is negligible and shows up on the neighboring C atoms only. On the other hand, the g anisotropy is induced by additional fields along x and y directions within the plane of σ skeleton

TABLE I. Summary of g values and linewidths as obtained from simulations.

g value	Linewidth (mT)
P⁺	
$g_{\parallel} = 2.0034(1)$	0.8
$g_{\perp} = 2.0024(1)$	0.5
I₂ doped MDMO-PPV	
$g_{\parallel} = 2.0033(1)$	0.8
$g_{\perp} = 2.0023(1)$	0.6
PCBM⁻	
$g_x = 2.0003(1)$	0.23
$g_y = 2.0001(1)$	0.13
$g_z = 1.9982(1)$	0.88

and not along the perpendicular z direction. An anisotropic axial g matrix (g_{\parallel} and g_{\perp}) of P⁺ on the conjugated segment is therefore expected and is seen in LEPR.

The negatively charged C₆₁ has rhombic symmetry with $g_x = 2.0003(1)$, $g_y = 2.0001(1)$, and $g_z = 1.9982(1)$. Again, the deviation of the g factor value from the free-electron value is due to the fact that the orbital angular moment is not completely quenched. Such g values below the free-electron value form a distinct feature of the C₆₀ molecule as observed in solution and in solid state.^{23,24,26–28} Due to a dynamical Jahn-Teller effect accompanying the structural molecular deformation, the isotropic nature of the icosahedral C₆₀ molecule is distorted after formation of the singly negatively charged C₆₀ ion, resulting in an axial or even lower symmetry.²⁹ Our measurements show that this is also the case for the PCBM⁻ ion of PCBM, where, however, the high symmetry of the molecule is already decreased by the bond to the phenyl side chain prior to electron trapping. Furthermore, it was established that the line shape of the PCBM⁻ signal can be best simulated with rhombic and not with axial symmetry. A Lorentzian line shape was used in the fit. For both contributions to the LEPR spectrum, the line widths and appropriate g values are given in Table I.

From our experiments, it is not possible to determine the distance between the positive and negative polarons. However, they are sufficiently apart from each other that no spin-spin interactions, such as triplet formation or exchange interactions, were observed. Spin-spin exchange interactions may influence the line shape and the linewidth. In this perspective the investigation of the doped polymer described later in this paper brings more insight.

Both EPR-active species, i.e., spins localized on the polymer backbone and on the methanofullerene, have strongly different spin lattice relaxation time T_1 , which shows up in a different microwave power saturation behavior. Saturation is easily reached for the P⁺ signals, while for the PCBM⁻ spectrum it was still absent at the highest available power. This difference was shown already to be a helpful tool to distinguish between the species in the X-band, where the g factor resolution of signals is insufficient.¹⁹ Therefore we

conclude that spin exchange, which would equalize T_1 of both types of photogenerated spins, is not a dominant relaxation process.

In our W-band measurements, performed in high magnetic fields, an additional effect was observed compared to X-band. Upon increasing microwave power the line shape of the P⁺—initially Gaussian—appears to be more complicated and in the end takes the shape of the absorption spectrum [see Fig. 3(b)] instead of its first derivative. In contrast to what one expects under saturation conditions, the resonance does not decrease in amplitude, due to a fast passage effect. The reader is referred to Ref. 31 for examples and general conditions in which the effect can occur. One of them is inhomogeneous broadening of the transition, which is consistent with our best fit of the P⁺ EPR line shape using a Gaussian line shape (see above). The phase difference between the modulated signal and the reference has to be zero to avoid the effect but in practice this is hard to maintain. The effect was not observed with EPR spectrometers that operate at lower microwave frequency (see, for example, Ref. 19) since the relaxation time (and hence the saturation) increases with the operating frequency. Caused by the conditions of experiment, the fast passage effect may be useful for comparative analysis of the relaxation times.

A temperature dependence of the EPR intensity was measured, however, only in a small temperature interval from 100 to 160 K. At $T = 100$ K, the concentrations of both radicals were found to be of the same order of magnitude, as derived from comparison of their double-integrated intensities in nonsaturated conditions. The decrease of the intensities at increasing temperatures is in general agreement with the findings from the X-band EPR study:¹⁹ a bimolecular annihilation process is involved, but a net signal of the P⁺ radicals remains at high temperatures. The latter points to the presence of EPR silent trapping sites for the negative polaron in the composite material.¹⁹

To corroborate the assignment of the low-field transition to P⁺, another experiment was performed on the MDMO-PPV. One can deliberately create positive polarons on the polymer by doping it with an acceptor. In this particular case molecular iodine I₂ was used. After the polymer was dried from solution in the EPR sample tube, it was subjected to sublimated I₂. The sample was measured at 100 K. At a low degree of doping (the sample was exposed approximately 10 sec to I₂ vapor), the axial symmetry is again clearly visible (Fig. 4). Also the g values agree, within the experimental error, to the one found for the P⁺ spectrum in the composite. At higher doping levels, reached after exposure time to the doping agent of 5 min and 4 h, only a single EPR line is detected. Moreover, the linewidth is about 1.05 and 1.33 mT, respectively, much broader than that obtained in the case of composites (0.5 and 0.8 mT, see Table I) where the g_{\parallel} and g_{\perp} transitions could be resolved [see Fig. 3(a)]. Using the same g parameters (Table I) and increasing the linewidth to 1 mT or more in the simulation, we obtain a single EPR line as is seen in this experiment. The broadening of the EPR transitions is most likely due to dipole-dipole interaction between charged polarons. The dipole-dipole linewidth can be estimated by $\Delta B_{dd} = \mu_B / R_0^3 = 4/3 \pi \mu_B n_P$, where μ_B is Bohr magneton, R_0 is distance between dipoles and is proportional

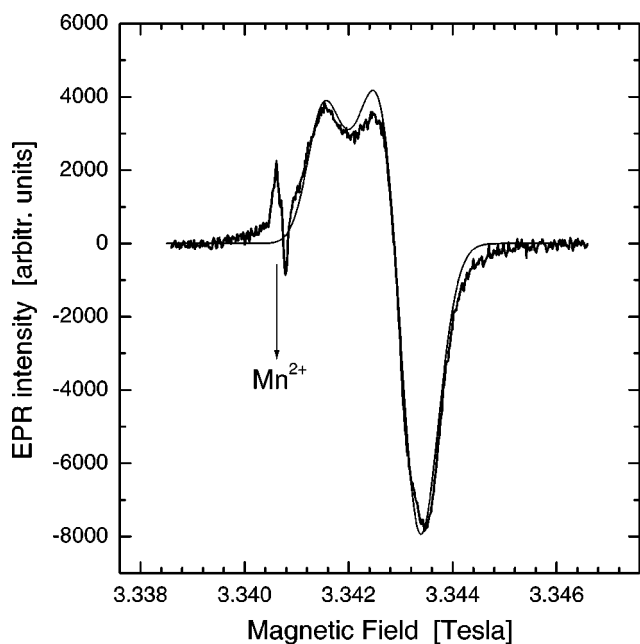


FIG. 4. EPR spectrum of I_2 -doped MDMO-PPV ($T=100$ K $P_{\mu w}=5 \times 10^{-6}$ mW). The thin line is the simulation.

to the polaron concentration n_P on the polymer chain. If one calculates the dipolar distance in the case of $\Delta B_{dd}=1$ mT, one obtains $R_0 \approx 10$ Å.

IV. CONCLUSIONS

Our high-frequency LEPR experiments on the MDMO-PPV/PCBM composite lead to the following conclusions.

After excitation of the composite in the absorption band of the conjugated polymer, two paramagnetic species are formed and can be clearly resolved in the LEPR spectrum: the positive polaron on the polymer backbone, P^+ with axial symmetry, and the negatively charged methanofullerene with rhombic symmetry. The g values are determined as follows: (i) $g_{\parallel}=2.0034(1)$ and $g_{\perp}=2.0024(1)$ for the positive polaron—chemical doping of MDMO-PPV by molecular iodine resulted in spectra with identical g values, giving extra proof for this assignment—and (ii) $g_x=2.0003(1)$, $g_y=2.0001(1)$, and $g_z=1.9982(1)$ for the PCBM radical anion. Both radicals have strongly different spin-lattice relaxation behavior which is in accordance with previous observations in X-band EPR and seems to be an intrinsic feature of the radicals in these composites. For the P^+ this gives rise to a rapid passage effect at higher microwave power.

ACKNOWLEDGMENTS

This work was supported by the Fund for Scientific Research, Flanders (FWO). The Laboratory for Experimental Condensed Matter Physics (ECM) of the University of Antwerp acknowledges financial support from the Flemish Government in the concerted research action (GOA 99/3/34) Multidisciplinary Spectroscopic Investigation of Organic Materials and Biomolecules. V.D. gratefully acknowledges financial support by German Research Council (DFG) (Grant PA378/3). We thank N. S. Sariciftci (LIOS), C. J. Brabec (LIOS), O. Poluektov (Argonne National Laboratory), W. Geens (IMEC), and J. Parisi (University of Oldenburg) for helpful discussions and experimental help.

- ¹W.A. Gazotti, A.F. Nogueira, E.M. Girotto, L. Micaroni, M. Martin, S. das Neves, and M.-A. De Paoli, in *Handbook of Advanced Electronic and Photonic Materials and Devices*, Light Emitting Diodes, Lithium Batteries and Polymer Devices Vol. 10, edited by H.S. Nalwa (Academic Press, San Diego, 2001), Chap. 2.
- ²N.F. Colaneri, D.D.C. Bradley, R.H. Friend, P.L. Burn, A.B. Holmes, and C.W. Spangler, *Phys. Rev. B* **42**, 11 670 (1990).
- ³J.W.P. Hsu, M. Yan, T.M. Jedju, L.J. Rothberg, and B.R. Hsieh, *Phys. Rev. B* **49**, 712 (1994).
- ⁴M. Yan, L.J. Rothberg, F. Papadimitrakopoulos, M.E. Galvin, and T.M. Miller, *Phys. Rev. Lett.* **72**, 1104 (1994).
- ⁵A.R. Brown, K. Pichler, N.C. Greenham, D.D.C. Bradley, R.H. Friend, and A.B. Holmes, *Chem. Phys. Lett.* **210**, 61 (1993).
- ⁶L.S. Swanson, P.A. Lane, J. Shinar, and F. Wudl, *Phys. Rev. B* **44**, 10 617 (1991).
- ⁷Z.V. Vardeny and X. Wei, *Mol. Cryst. Liq. Cryst.* **256**, 465 (1994).
- ⁸V. Dyakonov, G. Rösler, M. Schwoerer, S. Blumstengel, and K. Lüders, *J. Appl. Phys.* **79**, 1556 (1996).
- ⁹N.C. Greenham, J. Shinar, J. Partee, P.A. Lane, O. Amir, F. Lu, and R.H. Friend, *Phys. Rev. B* **53**, 13 528 (1996).
- ¹⁰V. Dyakonov, G. Rösler, M. Schwoerer, and E.L. Frankevich, *Phys. Rev. B* **56**, 3852 (1997).
- ¹¹V. Dyakonov, in *Primary Photoexcitations in Conjugated Polymers*, edited by N.S. Sariciftci (World Scientific, Singapore, 1997), Chap. 10.
- ¹²E.L. Frankevich, A.A. Lymarev, I. Sokolik, F.E. Karasz, S. Blumstengel, R.H. Baughman, and H.H. Hörhold, *Phys. Rev. B* **46**, 9320 (1992).
- ¹³K. Murata, Y. Shimoi, S. Abe, S. Kuroda, T. Noguchi, and T. Ohnishi, *Chem. Phys.* **227**, 191 (1998).
- ¹⁴C.H. Lee, G. Yu, D. Moses, K. Pakbaz, C. Zhang, N.S. Sariciftci, A.J. Heeger, and F. Wudl, *Phys. Rev. B* **48**, 15 425 (1993).
- ¹⁵B. Kraabel, C.H. Lee, D. McBranch, D. Moses, N.S. Sariciftci, and A.J. Heeger, *Chem. Phys. Lett.* **213**, 389 (1993).
- ¹⁶B. Kraabel, D. McBranch, N.S. Sariciftci, D. Moses, and A.J. Heeger, *Phys. Rev. B* **50**, 18 543 (1994).
- ¹⁷N.S. Sariciftci, L. Smilowitz, A.J. Heeger, and F. Wudl, *Science* **258**, 1474 (1992).
- ¹⁸R.A.J. Janssen, J.C. Hummelen, K.H. Lee, K. Pakbaz, N.S. Sariciftci, A.J. Heeger, and F. Wudl, *J. Chem. Phys.* **103**, 788 (1995).
- ¹⁹V. Dyakonov, G. Zorinians, M. Scharber, C.J. Brabec, R.A.J. Janssen, J.C. Hummelen, and N.S. Sariciftci, *Phys. Rev. B* **59**, 8019 (1999).

- ²⁰V.I. Krinichnyi, *Synth. Met.* **108**, 173 (2000).
- ²¹D.A. Holiday, P.L. Burn, D.D.C. Bradley, R.H. Friend, O.M. Gelsen, A.B. Holmes, A. Kraft, J.H.F. Martens, and K. Pichler, *Adv. Mater.* **5**, 40 (1993).
- ²²D. Dick, X. Wei, S. Jeglinski, R.E. Benner, Z.V. Vardeny, D. Moses, V.I. Srdanov, and F. Wudl, *Phys. Rev. Lett.* **73**, 2760 (1994).
- ²³R.W. Lof, M.A. van Veenendaal, B. Koopmans, H.T. Jonkman, and G.A. Sawatzky, *Phys. Rev. Lett.* **68**, 3924 (1992).
- ²⁴P.-M. Allemand, K.C. Khemani, A. Koch, F. Wudl, K. Holzer, S. Donovan, G. Grüner, and J.D. Tomson, *Science* **253**, 301 (1991).
- ²⁵K. Möbius, *Z. Naturforsch. A* **20A**, 1093 (1965).
- ²⁶D. Dubois, M.T. Jones, and K.M. Kadish, *J. Am. Chem. Soc.* **114**, 6446 (1992).
- ²⁷J. Stinchcombe, A. Penicaud, P. Bhyrappa, P.D.W. Boyd, and C.A. Reed, *J. Am. Chem. Soc.* **115**, 5212 (1993).
- ²⁸E. Tossati, N. Manini, and O. Gunnarsson, *Phys. Rev. B* **54**, 17 184 (1996).
- ²⁹W. Bietsch, J. Bao, J. Lüdecke, and S. van Smaalen, *Chem. Phys. Lett.* **324**, 37 (2000).
- ³⁰EPR-NMR program, developed by M.J. Mombourquette, J.A. Weil, and D.G. McGavin, University of Saskatchewan.
- ³¹C. Mailer and C.P.S. Taylor, *Biochim. Biophys. Acta* **322**, 195 (1973).
- ³²B. Henderson and J.E. Wertz *Defects in the Alkaline Earth Oxides: With Application to Radiation Damage and Catalysis* (Taylor & Francis, London, 1977).